Hemilabile Quinone Ligands Enable Nickel-Catalyzed C–S(Alkyl) Bond Formation in the Carbosulfenylation of Unactivated Alkenes

Zi-Qi Li[†], Turki, M. Alturaifi[§], Matthew V. Joannou[‡], Peng Liu[§*], and Keary M. Engle[†*]

[†] Department of Chemistry, Scripps Research, 10550 North Torrey Pines Road, La Jolla, California 92037, United States

[§] Department of Chemistry, University of Pittsburgh, 219 Parkman Avenue, Pittsburgh, Pennsylvania 15260, United States

[‡] Chemical Process Development Bristol Myers Squibb, One Squibb Drive, New Brunswick, New Jersey 08903, United States

ABSTRACT: A three-component coupling approach towards structurally complex dialkylsulfides is described via the nickel-catalyzed 1,2-carbosulfenylation of unactivated alkenes with organoboron nucleophiles and alkylsulfenamide (N–S) electrophiles. Efficient catalytic turnover is facilitated using a tailored N–S electrophile containing an *N*-methyl methanesulfonamide leaving group, allowing catalyst loadings as low as 1 mol%. Regioselectivity is controlled by a collection of monodentate, weakly coordinating native directing groups, including sulfonamides, amides, sulfinamides, phosphoramides, and carbamates. Key to the development of this transformation is the identification of quinones as a family of hemilabile and redox-active ligands that tune the steric and electron properties of the metal throughout the catalytic cycle. DFT results show that the duroquinone (DQ) ligand adopts different coordination modes in different elementary steps of the Ni-catalyzed 1,2-carbosulfenylation—binding as an X-type redox-active durosemiquinone radical anion to promote alkene migratory insertion with a less distorted square planar Ni(II) center, while binding as an L-type ligand to promote N–S oxidative addition at a more electron-rich Ni(I) center.

INTRODUCTION

Organosulfur compounds possess unique properties that give rise to applications in medicinal chemistry,[1] material science,[2] and other scientific fields. Organosulfides, in which sulfur is in the +2 oxidation state, can be readily converted into sulfoxides, sulfones, and sulfoximines, which are likewise important functional groups in drug discovery[3] and other realms. Traditional methods for transition-metal-catalyzed two-component C–S bond formation[4] can be categorized into two main redox paradigms. The Buchwald–Hartwig-type C–S coupling of organohalide electrophiles and organothiol nucleophiles represents a classical method for constructing C(sp^2)–S bonds.[5–6] Recently, there has been a growing interest in umpolung C–S couplings. These reactions utilize electrophilic sulfur reagents,[4h] which have favorable features, including their structural tunability, reduced tendency towards catalyst poisoning, and odorless nature (Scheme 1A). On this front, notable advancements have been achieved in transition-metal-catalyzed C–H functionalization reactions using electrophilic sulfonylthioate[7], sulfenamide[8], disulfide[9], and other sulfur surrogates[10].

While umpolung C–S coupling has primarily focused on C(sp^2)–S(Aryl) bond formation[7–11], there is growing interest in gaining access to unexplored regions of C(sp^3)-rich organosulfur chemical space, specifically, broadening the scope to include aliphatic carbon (C(sp^3)), and alkylsulfenyl (S(Alkyl)) reagents (Scheme 1B). A greater fraction of C(sp^3) atoms within a molecule makes it more three-dimensional, a critical feature for contemporary drug discovery.[12] Whereas several recent studies have described catalytic C(sp^3)–S(Aryl) bond formation, for example using radical-based approaches,[7b] methods that bring about C(sp^3)–S(Alkyl) bond formation remain comparatively rare.[13] In this work, we sought to develop a general method for the construction of C(sp^3)–S(Alkyl) bond through reagent and ligand design.

Scheme 1. Background and Synopsis of Current Work

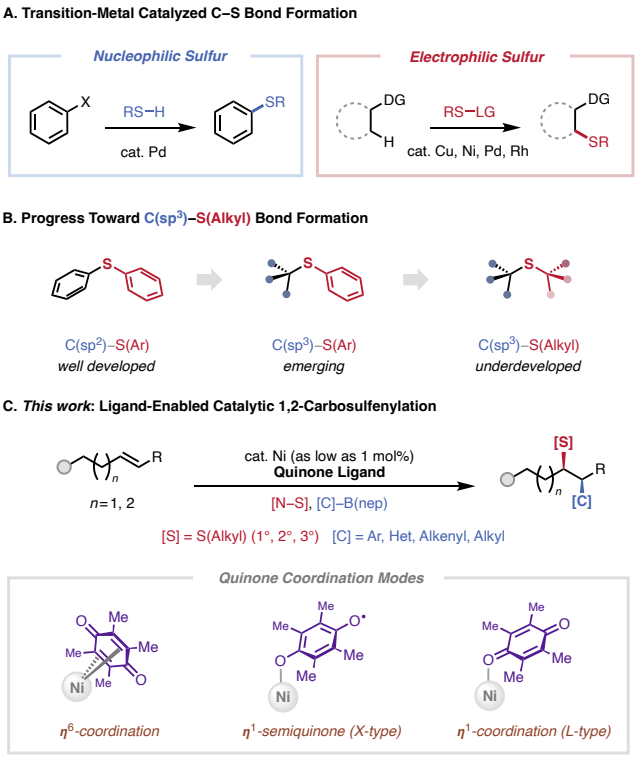

Transition-metal catalyzed 1,2-functionalization of alkenes has emerged as a powerful means to quickly construct densely functionalized products. These transformations allow programmable introduction of two distinct functional groups onto an alkene in a regio– and diastereoselective fashion.[14–16] Recently, our group reported a nickel-catalyzed *syn*-selective 1,2-carbosulfenylation reaction of simple unactivated alkenes for the construction of *vicinal* C(sp^3)–C((Hetero)Aryl) and C(sp^3)–S(Ar) bonds.[17] A reliable method extending the sulfur

https://doi.org/10.26434/chemrxiv-2023-ft0bn **ORCID:** https://orcid.org/0000-0003-2767-6556 Content not peer-reviewed by ChemRxiv. **License:** CC BY-NC-ND 4.0

electrophile scope to encompass 1°, 2°, and 3° S(Alkyl) groups, and simultaneously augmenting the carbon nucleophile scope to alkenyl and alkyl groups would round out synthetic capabilities within this family of reactions. However, attempts to directly apply the N–S reagent tuning strategy from our prior work to S(Alkyl) electrophiles were unsuccessful. Consequently, we sought to identify an ancillary ligand to enable productive three-component coupling with S(Alkyl) coupling partners.

For decades, quinones have been employed as (co)oxidants[18,19] and/or promoters of reductive elimination in transition-metal catalysis.[20] Our laboratory has recently studied quinones as electron-deficient diene ligands in the context of air-stable Ni(0) pre-catalysts.[21] With the commercialization of Ni(COD)(DQ) (DQ = duroquinone), an increasing number of studies have noted similar and in some cases improved reactivity compared to $Ni(COD)_2$.[22] Nevertheless, a holistic understanding of the coordination behavior and mechanistic role of (duro)quinone ligands remains elusive. Herein, we report the discovery of quinones as hemilabile, redox-active ligands that adopt different binding poses in order to promote individual elementary steps in the nickel-catalyzed 1,2-carbosulfenylation reaction.

Table 1. Electrophile, Nucleophile, and Alkenyl Sulfonamide Scope[a]

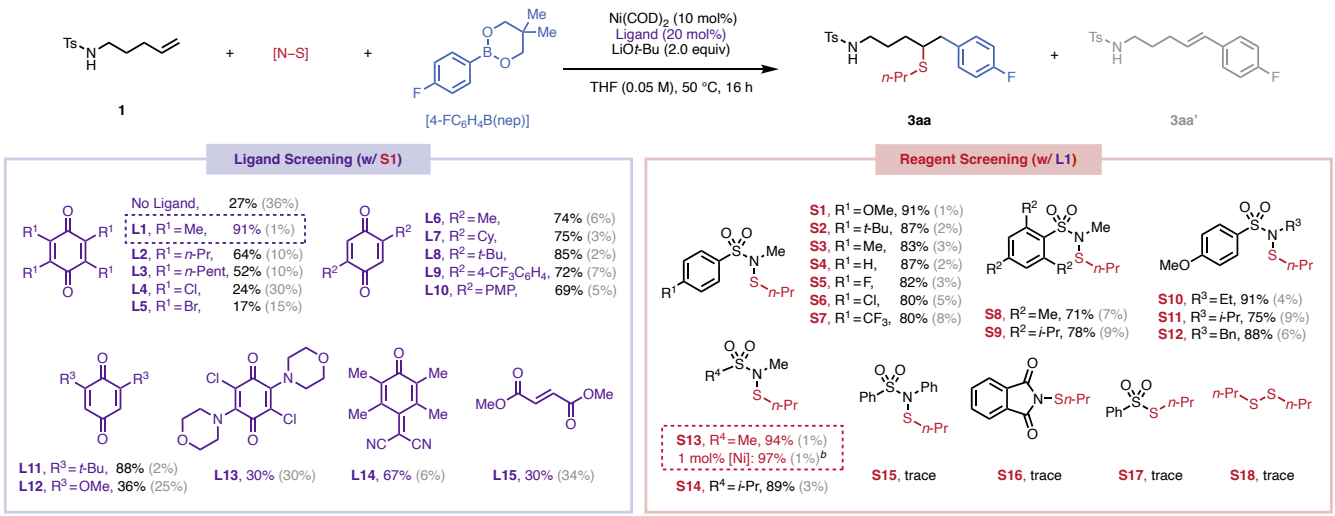

[a]Reactions performed on 0.1 mmol scale. $Ni(COD)_2$/**1**/Ligand/LiO*t*-Bu/[N–S]/4-F-C_6H_4B(nep) = 0.01/0.1/0.02/0.2/0.2/0.2 (mmol). THF (2.0 mL). Percentage yields represent ^1H NMR yields with benzyl 4-fluorobenzoate as internal standard. Yield in parenthesis represent ^1H NMR yields of byproduct **3aa'**. trace=<5%. [b]$Ni(COD)_2$/**1**/Ligand/LiO*t*-Bu/[N–S]/4-F-C_6H_4B(nep) = 0.001/0.1/0.005/0.2/0.15/0.2 (mmol). THF (1.0 mL). See supporting information for details.

RESULTS AND DISCUSSION

Reaction discovery. To initiate the investigation, we selected alkenyl sulfonamide **1**, 4-fluorophenylboronic acid neopentyl glycol ester, and *n*-propylsulfenamide **S1** containing a 4-methoxy-*N*-methylbenzenesulfonamide leaving group as the three model reactants (Table 1).[17a] In preliminary experiments with $Ni(COD)_2$ as the precatalyst without added ligand, a maximum yield of 27% of the desired 1,2-carbosulfenylated **3aa** product was obtained, accompanied by 37% yield of the corresponding oxidative Heck byproduct **3aa'**. These results could not be improved despite extensive attempts to optimize the structure of the N–S reagent and reaction conditions. Thus, we turned attention toward ancillary ligands to improve product yield and suppress oxidative Heck byproduct formation. To our delight, quinones were identified as effective ligands for both purposes. Tetrasubstituted quinones were first evaluated, with duroquinone (DQ, **L1**) giving the highest yield of 91% and minimizing oxidative Heck byproduct formation. Increasing the steric encumbrance (**L2**–**L3**) only gave moderate product yield and increased byproduct formation. More electron-deficient and more oxidizing quinones, such as chloranil and bromoanil (**L4**–**L5**), hampered the reaction, potentially due to electron transfer between catalyst and ligand.[23] Subsequently, 2,5-disubstituted quinone ligands with alkyl (**L6**–**L8**) and aryl (**L9**–**L10**) groups were tested, giving moderate to good yield and less than 10% byproduct formation. Steric and electronic modifications to the substituents at these positions exhibited only a minor effect on reactivity. Excellent results were obtained with 2,6-di-*tert*-butylquinone (**L11**) as ligand, providing a potential alternative ligand to DQ. On the other hand, a more electron-rich 2,6-dimethoxy ligand (**L12**) resulted in significantly diminished yield and substantial oxidative Heck byproduct formation. Similar results were obtained with a 2,5-dichloro-3,6-dimorpholino ligand (**L13**). Dicyano *para*-quinone methide (**L14**) gave moderate yield when used as ligand. Other electron-deficient olefin ligands, such as dimethyl fumarate (DMFU, **L15**), furnished modest yield (30%) with more byproduct formation, underscoring the unique effectiveness of quinone ligands (see supporting information for detail). Pre-ligation of the DQ ligand to the nickel center led to slightly lower yield (see Supporting Information for details).

With DQ as the ligand, we next evaluated N–S reagents containing different leaving groups. Across sulfonamide leaving groups with different steric and electronic properties (**S1**–**S12**); yields of the 1,2-carbosulfenylated product consistently exceeded 70% with less than 10% byproduct formation. Minor detrimental effects were noted with electron-withdrawing groups on the aryl ring (**S5**–**S7**) and with sterically bulky substituents on either the arylsulfonyl or the *N*-alkyl moieties (**S8**–**S9**, **S11**). The best yield and selectivity were obtained using **S13**, which features an *N*-methyl methansulfonamide leaving group. At 10 mol% catalyst loading, 94% yield of **3aa** was recorded. Whereas other N–S reagents (e.g., **S1**) required catalyst loadings of 10 mol% for high yield, with N–S reagent **S13** and DQ as the ligand, the catalyst loading could be lowered to 1 mol% without a drop in yield (see

https://doi.org/10.26434/chemrxiv-2023-ft0bn **ORCID:** https://orcid.org/0000-0003-2767-6556 Content not peer-reviewed by ChemRxiv. **License:** CC BY-NC-ND 4.0

supporting information for detail). Consistent with our prior findings[17a], N–S reagents with *N*-phenyl benzene sulfonamide as leaving group (**S15**) failed to yield the desired product due to a substantially weaker N–S bond, whereas reagent with phthalimide as leaving group (**S16**) exhibited low solubility. Sulfenylthioate (**S17**) and disulfide (**S18**) reagents also did not form the desired product and could be recovered at the end of the reaction.

Table 2. Electrophile Scope[a]

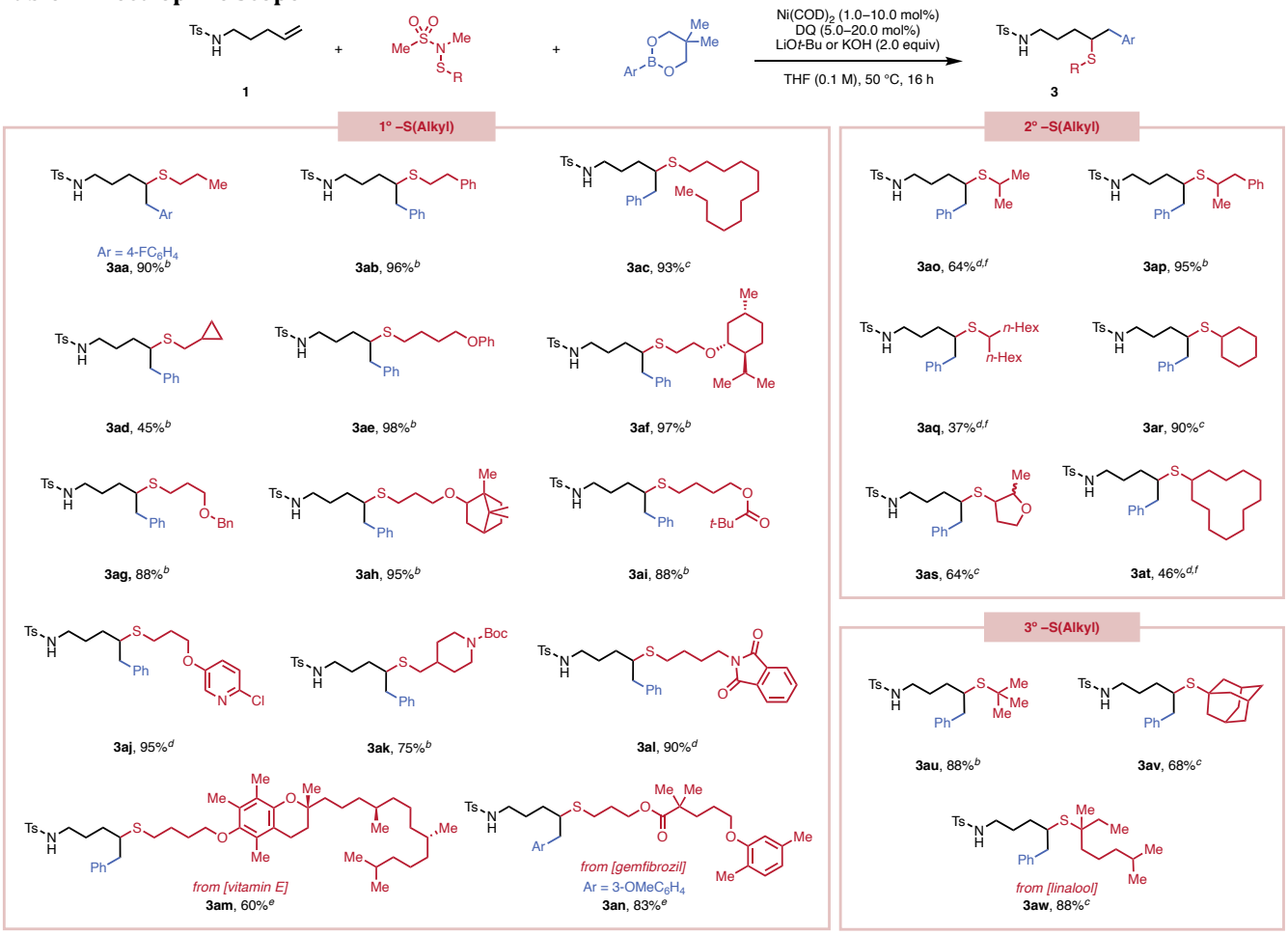

[a]Reactions performed on 0.1 mmol scale. Percentages represent isolated yields. [b]Reactions performed with N–S reagents bearing *N*-methylmethanesulfonamide as leaving groups at 1.0 mol% catalyst loading. [c]Reactions performed with N–S reagents bearing 4-methoxy-*N*-methylbenzenesulfonamide as leaving group at 2.0 mol% catalyst loading. In these cases an aromatic leaving group was selected to simplify purification of the product because *N*-methylmethanesulfonamide co-elutes with the product and is not UV-active. [d]Reactions performed with N–S reagents bearing *N*-methylmethanesulfonamide as leaving groups at 5.0 mol% catalyst loading. [e]Reactions performed with N–S reagents bearing *N*-methylmethanesulfonamide as leaving groups at 10.0 mol% catalyst loading. [f]Reactions performed with KOH (2.0 equiv) as base in place of LiO-*t*Bu (2.0 equiv).

Electrophile Scope. Having optimized a high-yielding and selective method, we turned attention to evaluating a series of primary, secondary, and tertiary alkylsulfenyl (–SAlkyl) electrophiles (Table 2). Primary alkylsulfenyl groups were first evaluated to understand reagent stability and functional group tolerance. It was found that various simple aliphatic –alkylsulfenyl groups could be incorporated without issue (**3aa–3ad**). In general, alkylsulfenyl groups with embedded oxygen and nitrogen substituents could also be incorporated in moderate to high yields, though in these cases the N–S reagent synthesis and stability merits discussion. Due to the use of electrophilic chlorinating agents such as SO_2Cl_2 and NCS in the preparation of N–S electrophiles (see supporting information for detail), nucleophilic functional groups prone to undergoing chlorination were not tolerated in standard synthetic procedure. For instance, attempts to prepare N–S electrophiles with free –OH, –NH, or electron-rich arenes were unfruitful. Moreover, the highly reactive N–S bond is susceptible to nucleophilic substitution. As a result, attenuating the nucleophilicity of any tethered nitrogen substituents through suitable protecting/blocking groups is required (**3aj–3al**) to avoid reagent decomposition. Less nucleophilic oxygen-based functional groups, however, were generally well tolerated (**3ae–3ai**, **3am–3an**). It is worth mentioning that carbonyl groups bearing acidic α-H atoms were incompatible potentially due to the in-situ generation of nucleophilic enolate moieties under the strong alkaline conditions. Therefore, only pivaloyl groups and derivatives thereof (**3al**, **3an**) were able to provide the corresponding products. The number of methylene ($–CH_2–$) units between sulfur and the heteroatom moiety could be varied between two and four without evident influence on the reaction outcome, giving **3ae–3an** in good to excellent yields. Testing the compatibility of the chemistry with more structurally complex, biologically relevant structures, as exemplified in vitamin E (**3am**) and gemfibrozil (**3an**) derivatives furnished the desired product in good yields, despite a higher catalyst loading is required. Subsequently, N–S reagents with secondary –SAlkyl functional groups were tested. Both acyclic (**3ao–3aq**) and cyclic (**3ar–3at**) secondary alkylsulfenyl reagents proved compatible, with a minor

https://doi.org/10.26434/chemrxiv-2023-ft0bn **ORCID:** https://orcid.org/0000-0003-2767-6556 Content not peer-reviewed by ChemRxiv. **License:** CC BY-NC-ND 4.0

adjustment of the base (from LiO*t*-Bu to KOH) proving necessary for selected acyclic alkylsulfenyl groups (**3ao**, **3aq**) and a cyclic alkylsulfenyl group with a large ring (**3at**). We hypothesize that this adjustment was required to accommodate the slightly higher conformational flexibility. Tertiary alkylsulfenyl groups also exhibited excellent reactivity, giving **3au**–**3aw** in good yields. To the best of our knowledge, transition-metal catalyzed installation of tertiary SAlkyl moiety with electrophilic sulfenylating reagents such as sulfonyl thiolates and disulfides remains scarcely reported due to challenging reagent activation.[7–11, 13]

Table 3. Nucleophile Scope[a]

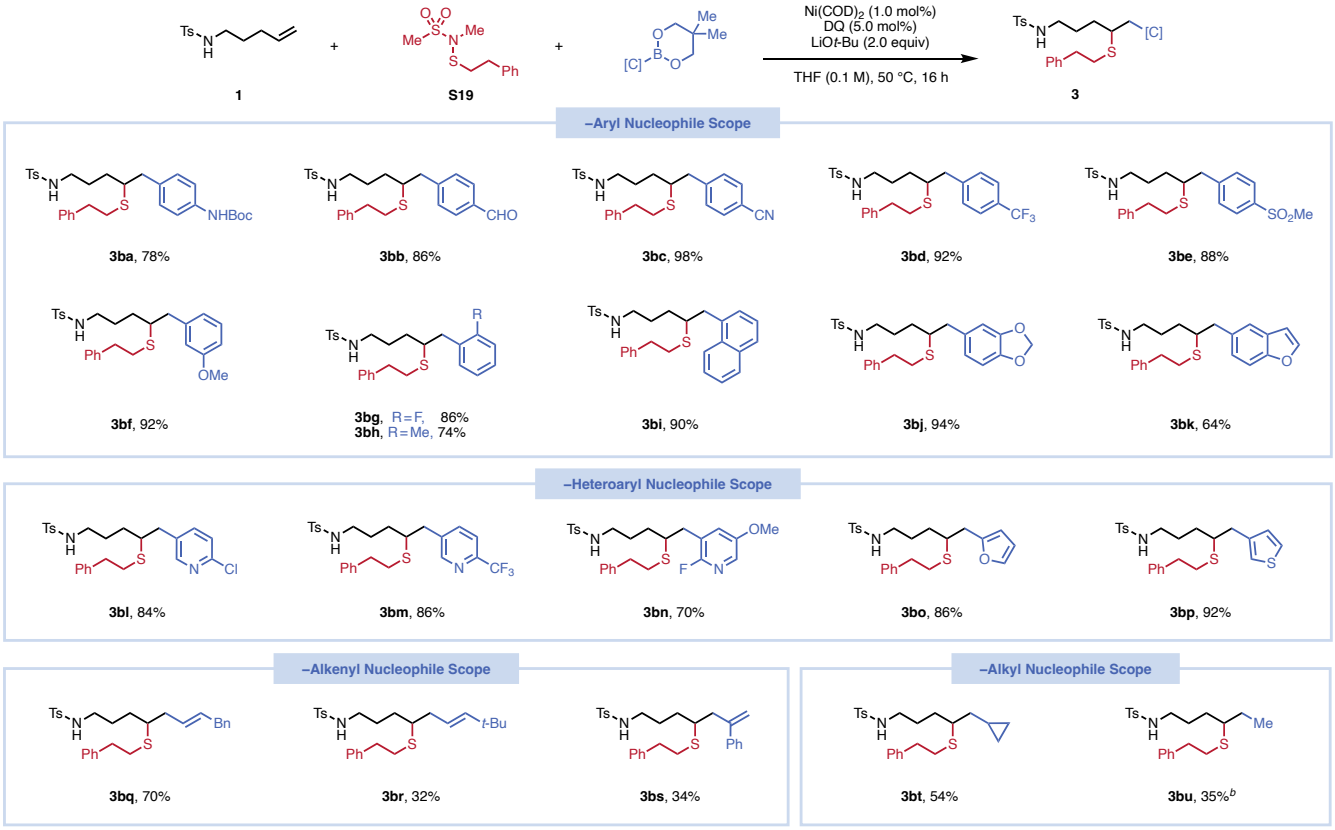

[a]Reactions performed on 0.1 mmol scale. Percentages represent isolated yields. [b]Reactions performed at 5.0 mol% catalyst loading. 5,5-diethyl-2-methyl-1,3,2-dioxaborinane was used as nucleophile.

Nucleophile Scope. Different organoboron nucleophiles were surveyed with **S13** as the standard sulfenylating reagent. To showcase the catalytic efficacy of the optimized procedure, all reactions were performed at 1 mol% catalyst loading. We were pleased to find that high turnover numbers were consistently obtained. Arylboron coupling partners with electronically distinct substituents (from electron-donating –NHBoc to electron withdrawing –SO_2Me) on the *para*- position all gave the corresponding products in good to excellent yields (**3ba**–**3be**). Potentially reactive or inhibitory groups, for instance –NHBoc (**3ba**), –CHO (**3bb**), and –CN (**3bc**), were all compatible. **3bf** with a –OMe substituent on the *meta*-position of carbon nucleophile was obtained in 92% yield. Furthermore, substituents on the *ortho*- position were well tolerated with no evident deterioration in product yield accompanying the increase in steric encumbrance (**3bg**–**3bi**). Aryl boronic esters with fused heterocycles, specifically benzodioxole and benzofuran moieties could be installed in 94% and 64% yield, respectively. We then committed to the exploration of heteroaryl carbon nucleophiles. Electron deficient pyridine-type nucleophiles could be introduced only in the presence of a substituent at 2-position to alleviate the coordinating property of the N(sp^2) atom (**3bl**–**3bn**). Meanwhile, electron rich heterocycles as exemplified by 2-furanyl and 3-thiofuranyl groups were also compatible (**3bo**–**3bp**), contributing to an extension of the carbon nucleophile library as compared to our previous carbosulfenylation protocol where only aryl– and electron-deficient heterocycles were demonstrated.[17a] To our delight, this extension can be further applied to alkenyl nucleophiles (**3bq**–**3bs**), and selected alkyl nucleophiles (**3bt**–**3bu**) with the latter being two rare examples using boron-based C(sp^3) nucleophiles. During the course of our study on the nucleophile scope, a higher C(sp^3) content by virtue of extending the coupling partner from –aryl, –heteroaryl, to –alkenyl and –alkyl were gradually exploited for the introduction of maximum four newly formed C(sp^3) centers, demonstrating high efficiency in constructing molecular complexity in concise manner.

Alkene Scope. A series of alkenyl sulfonamides with different substitution patterns were evaluated. When terminal alkenes were used, the reactivity could be maintained at low catalyst loading (**4a**–**4e**). Both benzenesulfonyl (**4a**–**4b**) and methanesulfonyl (**4c**) directing groups can furnish the corresponding products in prominent yields. While a branching on the β-position to the sulfonamide directing group resulted in moderate diastereoselectivity (**4d**), α-branching leads to significantly higher diastereoselectivity (**4e**). With internal alkenes as substrate, moderate to good yields and diastereoselectivities were obtained with a slightly higher catalyst loading (**4f**–**4k**). To illustrate the synthetic applicability of the described methodology, a removable sulfonamide directing group with 4-cyano substituent (Cs) was

https://doi.org/10.26434/chemrxiv-2023-ft0bn **ORCID:** https://orcid.org/0000-0003-2767-6556 Content not peer-reviewed by ChemRxiv. **License:** CC BY-NC-ND 4.0

tested based on the well-established derivatization protocol involving a deprotection/amination process. Excellent yield whilst moderate diastereoselectivity was obtained (**4h–4i**). A skipped diene at the γ,δ– and ζ,η–positions was used to examine the chemoselectivity of the reaction, giving exclusively γ,δ–carbosulfenylation product **4k**. An endocyclic alkenyl sulfonamide gave **4l** in 27% yield with >20:1 diastereoselectivity (see supporting information for detail). A double carbosulfenylation reaction of a symmetric diene was achieved by adding excessive (4.0 equiv) coupling partners, furnishing **4m** in 80% yield. We also explored the potential of expanding the compatible directing functionalities. Alkenyl amides with a variety of functional groups were tolerated, giving **4n–4p** in moderate yields. Additionally, phosphinic amide (**4q**), sulfinamide (**4r**), and carbamate (**4r**) were adequately reactive directing groups. Particularly, with Ellman's chiral sulfinamide as directing group, a 7:1 diastereoselectivity was obtained in **4r**. After extensive screening, we determined that a protic hydrogen atom was required for the reaction to proceed (see limitations). Non-directed alkenes, for instance, 1-phenylbutene and 1-dodecene were not operating, neither did alkenyl alcohols, azaheterocycles, or ketones.

Table 3. Alkene Scope[a]

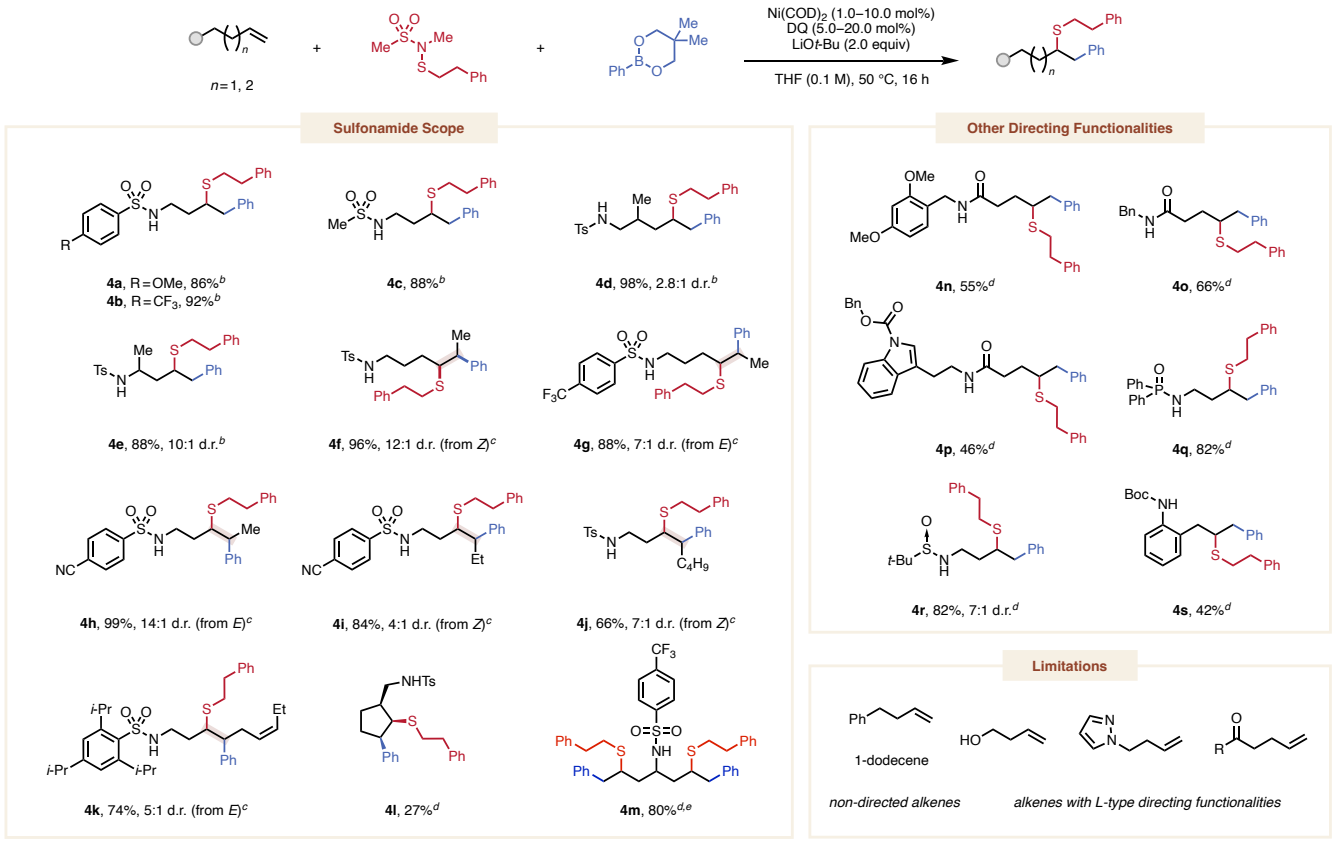

[a]Reactions performed on 0.1 mmol scale. Percentages represent isolated yields. [b]Reactions performed under 1 mol% catalyst loading. [c]Reactions performed under 5 mol% catalyst loading. [d]Reactions performed under 10 mol% catalyst loading. [e]Reaction performed with **S19** (4.0 equiv) and PhB(nep) (4.0 equiv).

Mechanistic Studies

The critical effect of quinone ligands in allowing integration of S(Alkyl) N–S electrophiles prompted us to investigate the origins of the enhanced reactivity using a combination of kinetics, density functional theory, and organometallic synthesis. First, we sought to understand the importance of in-situ ligation versus pre-ligation. To this end, we performed a series of initial rate experiments. While $Ni(COD)_2$ was only able to furnish 25% yield before catalyst deactivation, both pre-ligated Ni(COD)(DQ) and in-situ ligation of $Ni(COD)_2$ and duroquinone (DQ) gave excellent yield after extended reaction time (see Supporting Information for detail). However, an approximately twofold initial rate was observed with in-situ ligation, as in our standard conditions (Figure 1A). We rationalize these results on the basis that the Ni(I)/Ni(III) catalytic cycle requires an initial single-electron oxidation step that is more challenging from pre-ligated Ni(COD)(DQ) compared to $Ni(COD)_2$.

https://doi.org/10.26434/chemrxiv-2023-ft0bn **ORCID:** https://orcid.org/0000-0003-2767-6556 Content not peer-reviewed by ChemRxiv. **License:** CC BY-NC-ND 4.0

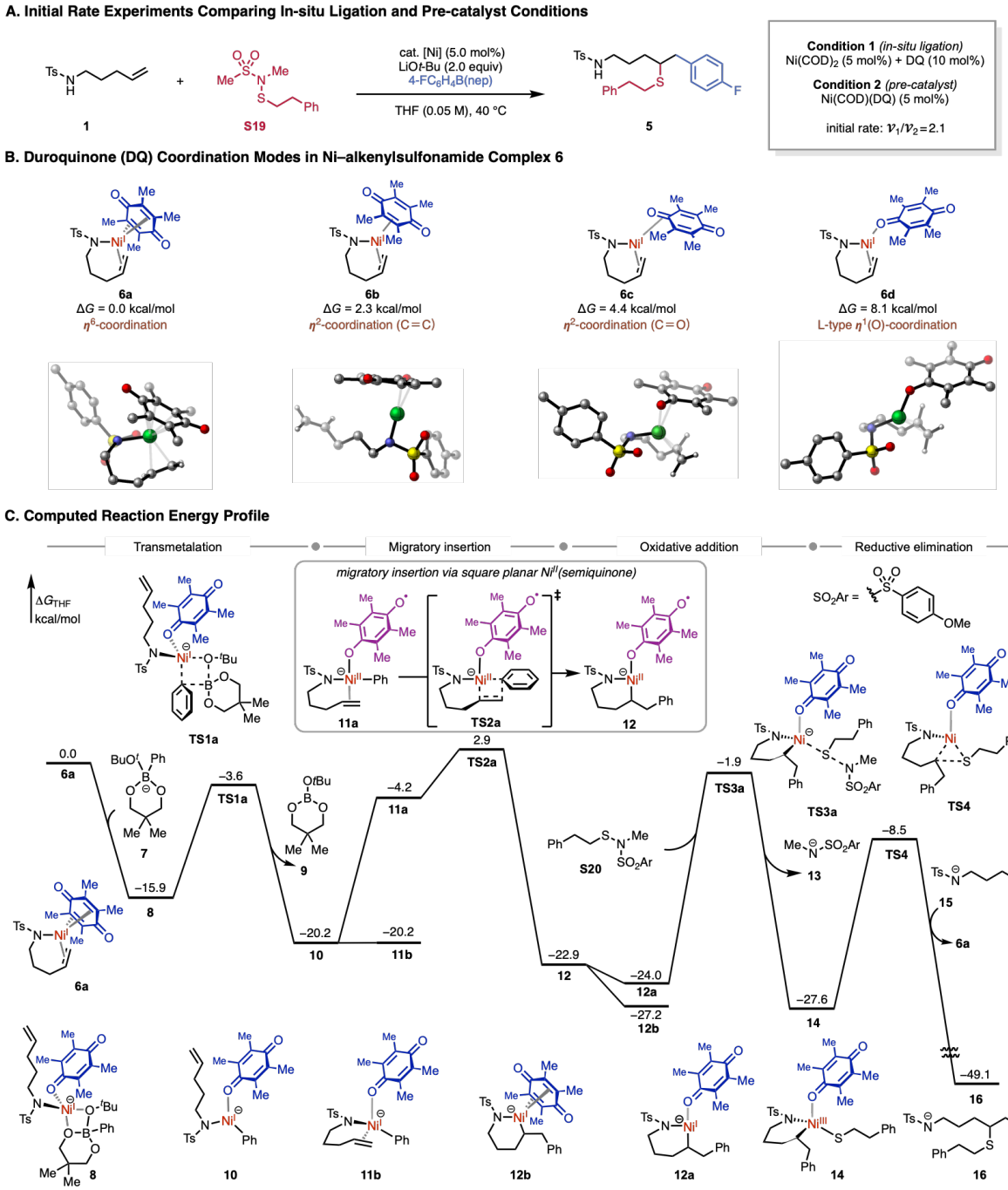

Figure 1. A) Initial rate experiments. B) Potential coordination modes of the hemilabile DQ ligand. C) Computed reaction energy profile of the Ni catalyzed 1,2-carbosulfenylation of alkene **1** with duroquinone ligand (**L1**). All Gibbs free energies are with respect to the Ni–alkenyl sulfonamide complex **6a** and phenyl boronate anion **7**.

To further understand the role of quinone ligand in this reaction, density functional theory (DFT) calculations were performed particularly to explore the diverse coordination modes between the nickel catalyst and the quinone ligand. Because Ni complexes in the proposed catalytic cycle[17a] have different oxidation states, numbers of *d* electrons, and distinct steric properties, we surmised that the DQ ligand may adopt different coordination modes to facilitate different elementary steps.[24] We carefully considered several possible DQ coordination modes (Figure 1B) for each intermediate and transition state in the reaction of alkenyl sulfonamide **1**, phenylboronic acid neopentyl glycol ester, and the N–S electrophile **S20**.[25] The most favorable intermediates and transition states involved in each elementary step are shown in the reaction free energy profile in Figure 1C. The electron-rich π-alkene sulfonamide–Ni(I)complex **6** prefers an η^6 DQ coordination mode, in which the Ni center is simultaneously coordinated to the six carbons of the quinone ring (Figure 1B). According to our computational studies, this η^6 coordination mode is thermodynamically more stable by at least 2.3 kcal/mol than other possible coordination modes such as the η^2(C=C) bound **6b**, the η^2(C=O) bound **6c**, and the η^1(O)-bound **6d**. Upon binding of **6a** with phenylboronate **7**, a tetrahedral complex **8** is formed where the DQ binds via an L-type η^1-coordination with the carbonyl oxygen. The coordination of alkenyl sulfonamide **1** leads to a faster transmetalation of the phenyl group to the nickel center, as the transmetalation from a Ni(I) complex without sulfonamide coordination results in a

https://doi.org/10.26434/chemrxiv-2023-ft0bn **ORCID:** https://orcid.org/0000-0003-2767-6556 Content not peer-reviewed by ChemRxiv. **License:** CC BY-NC-ND 4.0

higher activation barrier by 25.5 kcal/mol (Figure S1). After transmetalation via **TS1a**, a phenyl Ni(I) complex **10** is formed, which also involves an η^1(O) DQ coordination. After coordination of the alkenyl group of the sulfonamide substrate to the Ni(I) center, a tetrahedral complex **11b** is formed, which also favors η^1 coordination of the DQ carbonyl oxygen to the electron-rich Ni. However, alkene migratory insertion cannot occur directly with **11b**, as it would require a highly distorted structure from the tetrahedral geometry. Instead, **11b** must isomerize to a square planar complex **11a** prior to migratory insertion. The computed natural spin densities from the Natural Bond Orbital (NBO) method[26] and the Ni–O(DQ) distance indicate that **11a** has a Ni(II) center bound to the oxygen atom of an X-type durosemiquinone (DSQ) radical anion (Figure 2A). The relatively short Ni–O distance in **11a** (1.92 Å) is consistent with those in other Ni^{II}–semiquinone

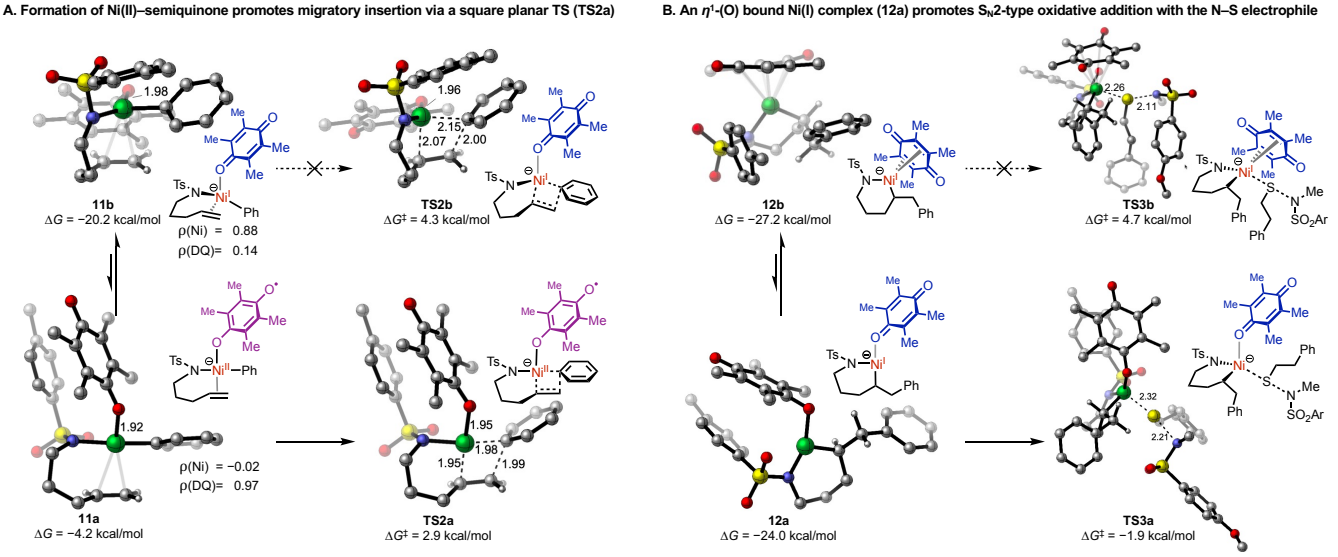

Figure 2. Preferred DQ coordination modes in (A) migratory insertion and (B) S_N2-type oxidative addition steps. Gibbs free energies are with respect to the Ni–alkenylsulfonamide complex **6a** and phenyl boronate anion **7.** Natural spin densities (ρ) were computed at the (U)ωB97X-D/6-311+G(d,p)–SDD(Ni)/SMD(THF) level of theory.

complexes.[27] Additionally, the computed spin densities in complex **11a** indicate that the unpaired electron is primarily located on the DQ ligand (0.97), consistent with the open-shell character of the durosemiquinone radical anion ligand. In contrast, the spin densities in complex **11b** localize the unpaired electron on the Ni atom (0.88), with a comparatively minor contribution from the DQ ligand. This is in line with the characteristics associated with an L-type ligand bound to a Ni(I) center. The square planar Ni^{II}(DSQ) complex **11a** undergoes facile migratory insertion via a square planar transition state **TS2a**, which is only 7.1 kcal/mol higher in energy than **11a** and 23.1 kcal/mol higher than the three-coordinated π-alkene Ni(I) intermediate **10**. By contrast, the direct migratory insertion from tetrahedral Ni(I) complex **11b** via **TS2b** requires a higher barrier (TS isomers with other DQ coordination modes are even less favorable. See Figure S3). **TS2a** directly leads to a T-shaped Ni^{II}(DSQ) complex **12**, which then isomerizes to form a more stable Ni(I) complex **12b** featuring an η^6-coordination to DQ, as in other electron-rich and relatively less hindered Ni(I) intermediates in the catalytic cycle (*e.g.*, **6a**). Before the subsequent oxidative addition step with the N–S reagent **S20**, the DQ binding mode changes again to an L-type η^1(O) coordination, leading to a more electron-rich and less sterically hindered Ni(I) center in **12a**. These electronic and steric properties in the η^1(O)-bound **12a** facilitate subsequent S_N2-type oxidative addition via **TS3a**, where the Ni center maintains a tetrahedral geometry with the L-type DQ ligand. On the other hand, the activation barrier of the oxidative addition from the sterically congested η⁶-coordinated **12b** via **TS3b** is 9.8 kcal/mol higher in energy than the activation barrier of **TS3a** via η¹(O)-bound **12a** (Figure 2B). Alternative oxidative addition pathways, including the η^2(C=C) coordination of DQ to Ni, are less stable than the oxidative addition via the η^1(O)-DQ coordination in **TS3a** (Figure S4). Finally, the C(sp^3)–S(alkyl) reductive elimination transition state **TS4** occurs via an η^1(O)-coordinated Ni(III) intermediate **14** to yield the 1,2-carbosulfenylation product.

Taken together, the DFT calculations indicate that DQ serves as a redox-active and hemilabile ligand to promote multiple elementary steps in the carbosulfenylation catalytic cycle. Although the DQ ligand often adopts an η^6 coordination mode in several intermediates involved in the catalytic cycle, it changes to an L-type η^1(O) coordination to accommodate the sterically encumbered transmetalation transition state (**TS1a**) and electronically promote the S_N2-type oxidative addition transition state with the N–S electrophile (**TS3a**). To mitigate the strain in the migratory insertion, an X-type semiquinone-bound Ni(II) complex is involved in a square planar migratory insertion transition state. Without these beneficial roles of DQ, multiple elementary steps can be more challenging. For example, the computed activation free energy of the migration insertion in the absence of the DQ ligand is 31.1 kcal/mol (see Figure S3), which is substantially higher than the activation free energy in the presence of DQ (Δ$G^‡$ = 23.1 kcal/mol, **TS2a**).

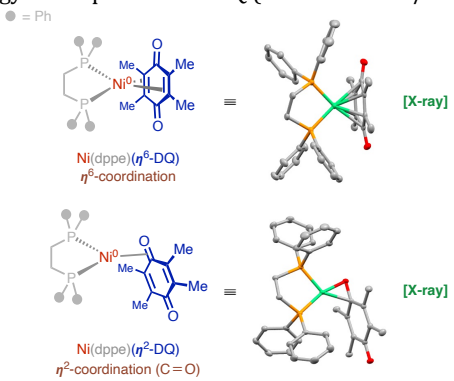

Figure 3. Two different coordination modes of Ni(dppe)(DQ) complex.

https://doi.org/10.26434/chemrxiv-2023-ft0bn **ORCID:** https://orcid.org/0000-0003-2767-6556 Content not peer-reviewed by ChemRxiv. **License:** CC BY-NC-ND 4.0

The hemilability of quinone ligands revealed by the computational study in several steps of the catalytic cycle prompted us to seek more structural evidence of this unique feature, which has not been previously documented in Ni(*para*-quinone) complexes to our knowledge.[21, 24–28] To this end, we treated Ni(COD)(DQ) with various bidentate ligands in an effort to study trends in coordination modes as a function of ligand properties. Whereas several weak-field ligands (e.g., bipy, 4,4'-*t*-Bu-bipy) led to formation of insoluble complexes that could not be characterized, clear ligand exchange was observed when a series of stronger-field bisphosphine ligands were used, revealing a distribution between η^6 and η^2 coordination modes in solution as a function of the ligand bite angle (see Supporting Information for detail). With 1,2-bis(diphenylphosphino)ethane (dppe), we were able to characterize both coordination modes in the solid state through X-ray crystallography (Figure 3). Though it should be emphasized that these ligands and conditions are not directly relevant to the catalytic conditions, the results nevertheless demonstrate multiple co-existing coordination modes under ambient conditions.[29]

CONCLUSION

In conclusion, a family of quinone ligands were identified to enable nickel-catalyzed 1,2-carbosulfenylation of unactivated alkenes using tailored [N–S] reagents as electrophiles. The synthetic versatility of the method stems from the broad scope of 1°, 2°, and 3° S(Alkyl) electrophiles and (hetero)aryl, alkenyl, and alkyl nucleophiles. A large array of unactivated alkenes with native functionalities could be functionalized in a highly regioselective manner. The mechanistic merit of the reaction originates from the identification of the unique quinone/nickel coordination modes. DFT calculations reveal that the DQ ligand acts as a redox-active and hemilabile agent to facilitate multiple elementary steps in the carbosulfenylation catalytic cycle by adopting different coordination modes. The ligand's ability to change coordination modes promotes sterically encumbered transmetalation and electronically accelerates S_N2-type oxidative addition transition states, contributing to the efficiency of the overall catalytic process.

ASSOCIATED CONTENT

Supporting Information. This material is available free of charge via the Internet at http://pubs.acs.org."
Experimental procedures, spectral, crystallographic data, computational details, and Cartesian coordinates of all computed structures (PDF)
NMR data (MNova format) (ZIP)

AUTHOR INFORMATION

Corresponding Author

Peng Liu – Department of Chemistry, University of Pittsburgh, Pittsburgh, Pennsylvania 15260, United States; orcid.org/0000-0002-8188-632X; Email: pengliu@pitt.edu

Keary M. Engle – Department of Chemistry, The Scripps Research Institute, La Jolla, California 92037, United States; orcid.org/0000-0003-2767-6556; Email: keary@ scripps.edu

Authors

Zi-Qi Li – Department of Chemistry, The Scripps Research Institute, La Jolla, California 92037, United States; orcid.org/0000-0002-1353-3004.

Turki M. Alturaifi – Department of Chemistry, University of Pittsburgh, Pittsburgh, Pennsylvania 15260, United States; https://orcid.org/0000-0002-6379-1669

Notes

The authors declare no competing financial interest.

ACKNOWLEDGMENT

This work was financially supported by the National Science Foundation (CHE-2102550), the Alfred P. Sloan Fellowship program, and the Camille Dreyfus Teacher-Scholar program. We thank Bristol Myers Squibb for a Graduate Fellowship (Z.-Q.L.). Dr. Jason Chen is acknowledged for HRMS analysis. Computational calculations were carried out at the University of Pittsburgh Center for Research Computing and the Advanced Cyberinfrastructure Coordination Ecosystem: Services & Support (ACCESS) program, supported by NSF award numbers OAC-2117681, OAC-1928147 and OAC-1928224. We thank Dr. Roger Sommer (Bristol Myers Squibb) for assistance with X-ray crystallography.

REFERENCES

(1) (a) Islardi, E. A.; Vitaku, E.; Njardarson, J. T. Data-mining for Sulfur and Fluorine: an Evaluation of Pharmaceuticals to Reveal Opportunities for Drug Design and Discovery. *J. Med. Chem.* **2014**, *57*, 2832−2842; (b) Zhao, C.; Rakesh, K. P.; Ravidar, L.; Fang, W. Y.; Qin, H. L. Pharmaceutical and Medicinal Significance of Sulfur (S(VI))-Containing Motifs for Drug Discovery: A Critical Review. *Eur. J. Med. Chem.* **2019**, *162*, 679−734. (c) Feng, M.; Tang, B.; Liang, S. H.; Jiang, X. Sulfur Containing Scaffolds in Drugs: Synthesis and Application in Medicinal Chemistry. *Curr. Top. Med. Chem.* **2016**, *16*, 1200−1216.

(2) Takimiya, K.; Osaka, I.; Mori, T.; Nakano, M. Organic Semiconductors Based on [1]Benzothieno[3,2-b][1]benzothiophene Substructure. *Acc. Chem. Res.* **2014**, *47*, 1493−1502.

(3) Modha, S. G.; Mehta, V. P.; van der Eycken, E. V. Transition Metal-catalyzed C−C bond formation via C−S bond cleavage: an overview. *Chem. Soc. Rev.* **2013**, *42*, 5042−5055.

(4) For reviews on transition metal-catalyzed C−S bond formation: (a) Beletskaya, I. P.; Ananikov, V. P. Transition-Metal-Catalyzed C−S, C−Se, and C−Te Bond Formation via Cross-Coupling and Atom-Economic Addition Reactions. *Chem. Rev.* **2011**, *111*, 1596−1636. (b) Lee, C. F.; Liu, Y. C.; Badsara, S. S. Transition-Metal-Catalyzed C−S Bond Coupling Reaction. *Chem-Asian J.* **2014**, *9*, 706−722. (c) Shen, C.; Zhang, P. F.; Sun, Q.; Bai, S. Q.; Hor, T. S. A.; Liu, X. G. Recent Advances in C-S Bond Formation via C−H Bond Functionalization and Decarboxylation. *Chem. Soc. Rev.* **2015**, *44*, 291−314. (d) Li, J. X.; Yang, S. R.; Wu, W. Q.; Jiang, H. F. Recent Developments in Palladium-Catalyzed C−S Bond Formation. *Org. Chem. Front.* **2020**, *7*, 1395−1417. (e) Sundaravelu, N.; Sangeetha, S.; Sekar, G. Metal-Catalyzed C−S Bond Formation Using Sulfur Surrogates. *Org. Biomol. Chem.* **2021**, *19*, 1459−1482. (f) Chen, Z. W.; Bai, R. K.; Annamalai, P.; Badsara, S. S.; Lee, C. F. The Journey of C−S Bond Formation from Metal Catalysis to Electrocatalysis. *New J. Chem.* **2021**, *46*, 15−38. (g) Kanchana, U. S.; Diana, E. J.; Mathew, T. V. Recent Trends in Nickel-Catalyzed C−S Bond Formation. *Asian J. Org. Chem.* **2022**, *11*, e202200038. (h) Wei, Y.-F.; Gao, W.-C.; Chang, H.-H.; Jiang, X. Recent Advances in Thiolation via Sulfur Electrophiles. *Org. Chem. Front.* **2022**, *9*, 6684−6707.

(5) For representative examples and mechanistic studies of palladium-catalyzed C−S bond formation with organothiols: (a) Hartwig, J. F. Carbon−Heteroatom Bond-Forming Reductive

https://doi.org/10.26434/chemrxiv-2023-ft0bn **ORCID:** https://orcid.org/0000-0003-2767-6556 Content not peer-reviewed by ChemRxiv. **License:** CC BY-NC-ND 4.0

Eliminations of Amines, Ethers, and Sulfides. *Acc. Chem. Res.* **1998**, *31*, 852−860. (b) Mann, G.; Baranano, D.; Hartwig, J. F.; Rheingold, A. L.; Guzei, I. A. Carbon−Sulfur Bond−Forming Reductive Elimination Involving sp−, sp^2−, and sp^3−Hybridized Carbon. Mechanism, Steric Effects, and Electronic Effects on Sulfide Formation. *J. Am. Chem. Soc.* **1998**, *120*, 9205−9219. (c) Baranano, D.; Hartwig, J. F. Carbon-Heteroatom Bond-Forming Reductive Elimination. Mechanism, Importance of Trapping Reagents, and Unusual Electronic Effects during Formation of Aryl Sulfides. *J. Am. Chem. Soc.* **2002**, *117*, 2937−2938. (d) Louie, J.; Hartwig, J. F. Transmetalation, Involving Organotin Aryl, Thiolate, and Amide Compounds. An Unusual Type of Dissociative Ligand Substitution Reaction. *J. Am. Chem. Soc.* **2002**, *117*, 11598−11599. (e) Fernandez-Rodríguez, M. A.; Shen, Q.; Hartwig, J. F. Highly Efficient and Functional-Group-Tolerant Catalysts for the Palladium-Catalyzed Coupling of Aryl Chlorides with Thiols. *Chemistry* **2006**, *12*, 7782−7796. (f) Fernandez-Rodríguez, M. A.; Shen, Q.; Hartwig, J. F. A General and Long-Lived Catalyst for the Palladium-Catalyzed Coupling of Aryl Halides with Thiols. *J. Am. Chem. Soc.* **2006**, *128*, 2180−2181. (g) Hartwig, J. F. Evolution of a Fourth-Generation Catalyst for the Amination and Thioetherification of Aryl Halides. *Acc. Chem. Res.* **2008**, *41*, 1534−1544. (h) Alvaro, E.; Hartwig, J. F. Resting State and Elementary Steps of the Coupling of Aryl Halides with Thiols Catalyzed by Alkylbisphosphine Complexes of Palladium. *J. Am. Chem. Soc.* **2009**, *131*, 7858−7868. (i) Fernandez-Rodríguez, M. A.; Hartwig, J. F. A General, Efficient, and Functional-Group-Tolerant Catalyst System for the Palladium-Catalyzed Thioetherification of Aryl Bromides and Iodides. *J. Org. Chem.* **2009**, *74*, 1663−1672. (j) Xu, J.; Liu, R. Y.; Yeung, C. S.; Buchwald, S. L. Monophosphine Ligands Promote Pd-Catalyzed C−S Cross-Coupling Reactions at Room Temperature with Soluble Bases. *ACS Catal.* **2019**, *9*, 6461−6466.

(6) For representative examples of C−S bond formation using other transition metals: (a) Wong, Y. C.; Jayanth, T. T.; Cheng, C. H. Cobalt-Catalyzed Aryl-Sulfur Bond Formation. *Org. Lett.* **2006**, *8*, 5613−5616. (b) Zhang, Y.; Ngeow, K. C.; Ying, J. Y. The First *N*-Heterocyclic Carbene-Based Nickel Catalyst for C−S Coupling. *Org. Lett.* **2007**, *9*, 3495−3498. (c) Correa, A.; Carril, M.; Bolm, C. Iron-Catalyzed S-Arylation of Thiols with Aryl Iodides. *Angew. Chem. Int. Ed.* **2008**, *47*, 2880−2883. (d) Sperotto, E.; van Klink, G. P.; de Vries, J. G.; van Koten, G. Ligand-Free Copper-Catalyzed C−S Coupling of Aryl Iodides and Thiols. *J. Org. Chem.* **2008**, *73*, 5625−5628. (e) Kabir, M. S.; Lorenz, M.; Van Linn, M. L.; Namjoshi, O. A.; Ara, S.; Cook, J. M. A Very Active Cu-Catalytic System for the Synthesis of Aryl, Heteroaryl, and Vinyl Sulfides. *J. Org. Chem.* **2010**, *75*, 3626−3643. (f) Venkanna, G. T.; Arman, H. D.; Tonzetich, Z. J. Catalytic C–S Cross-Coupling Reactions Employing Ni Complexes of Pyrrole-Based Pincer Ligands. *ACS Catal.* **2014**, *4*, 2941−2950. (g) Delcaillau, T.; Morandi, B. Nickel-Catalyzed Thiolation of Aryl Nitriles. *Chem-Eur. J.* **2021**, *27*, 11823−11826. (h) Zhang, F.; Wang, Y.; Wang, Y.; Pan, Y. Electrochemical Deoxygenative Thiolation of Preactivated Alcohols and Ketones. *Org. Lett.* **2021**, *23*, 7524−7528.

(7) Selected examples of C−H sulfenylation using sulfonyl thioesters as electrophiles: (a) Cai, W. Q.; Gu, Z. H. Selective Ortho Thiolation Enabled by Tuning the Ancillary Ligand in Palladium/Norbornene Catalysis. *Org. Lett.* **2019**, *21*, 3204−3209. (b) Mao, R.; Bera, S.; Turla, A. C.; Hu, X. Copper-Catalyzed Intermolecular Functionalization of Unactivated C(sp^3)–H Bonds and Aliphatic Carboxylic Acids. *J. Am. Chem. Soc.* **2021**, *143*, 14667−14675.

(8) (a) Saravanan, P.; Anbarasan, P. Palladium Catalyzed Aryl(alkyl)thiolation of Unactivated Arenes. *Org. Lett.* **2014**, *16*, 848−851. (b) Li, R. H.; Zhou, Y.; Yoon, K. Y.; Dong, Z.; Dong, G. B. Sulfenamide-enabled Ortho Thiolation of Aryl Iodides via Palladium/Norbornene Cooperative Catalysis. *Nat. Commun.* **2019**, *10*.

(9) Selected examples of various transition metal catalyzed C−H sulfenylation using disulfides as electrophiles: (a) Tran, L. D.; Popov, I.; Daugulis, O. Copper-Promoted Sulfenylation of sp^2 C−H Bonds. *J. Am. Chem. Soc.* **2012**, *134*, 18237−18240. (b) Iwasaki, M.; Iyanaga, M.; Tsuchiya, Y.; Nishimura, Y.; Li, W. J.; Li, Z. P.; Nishihara, Y. Palladium- Catalyzed Direct Thiolation of Aryl C−H Bonds with Disulfides. *Chem-Eur J.* **2014**, *20*, 2459−2462. (c) Yan, G. B.; Borah, A. J.; Wang, L. G. Efficient Silver-Catalyzed Direct Sulfenylation and Selenylation of Rich arenes. *Org. Biomol. Chem.* **2014**, *12*, 9557−9561. (d) Yang, Y. X.; Hou, W.; Qin, L. H.; Du, J. J.; Feng, H. J.; Zhou, B.; Li, Y. C. Rhodium-Catalyzed Directed Sulfenylation of Arene C−H Bonds. *Chem-Eur. J.* **2014**, *20*, 416−420. (e) Lin, C.; Li, D. Y.; Wang, B. J.; Yao, J. Z.; Zhang, Y. H. Direct ortho-Thiolation of Arenes and Alkenes by Nickel Catalysis. *Org. Lett.* **2015**, *17*, 1328−1331. (f) Li, M. L.; Wang, J. Cobalt-Catalyzed Direct C−H Thiolation of Aromatic Amides with Disulfides: Application to the Synthesis of Quetiapine. *Org. Lett.* **2018**, *20*, 6490−6493. Selected examples of C(sp^3)−H sulfenylation using directing auxiliary: (g) Wang, X.; Qiu, R. H.; Yan, C. Y.; Reddy, V. P.; Zhu, L. Z.; Xu, X. H.; Yin, S. F. Nickel-Catalyzed Direct Thiolation of C(sp^3)−H Bonds in Aliphatic Amides. *Org. Lett.* **2015**, *17*, 1970−1973. (h) Yan, S. Y.; Liu, Y. J.; Liu, B.; Liu, Y. H.; Zhang, Z. Z.; Shi, B. F. Nickel-Catalyzed Direct Thiolation of Unactivated C(sp^3)−H Bonds with Disulfides. *Chem. Commun.* **2015**, *51*, 7341−7344.

(10) Selected examples of C−H sulfenylation using sulfur surrogates: (a) Chen, F. J.; Liao, G.; Li, X.; Wu, J.; Shi, B. F. Cu(II)-Mediated C−S/N−S Bond Formation via C−H Activation: Access to Benzoisothiazolones Using Elemental Sulfur. *Org. Lett.* **2014**, *16*, 5644−5647. (b) Li, J. X.; Li, C. S.; Yang, S. R.; An, Y. N.; Wu, W. Q.; Jiang, H. F. Palladium-Catalyzed Oxidative Sulfenylation of Indoles and Related Electron-Rich Heteroarenes with Aryl Boronic Acids and Elemental Sulfur. *J. Org. Chem.* **2016**, *81*, 7771−7783. (c) Ge, X.; Sun, F. L.; Liu, X. M.; Chen, X. Z.; Qian, C.; Zhou, S. D. Combined Experimental/Theoretical Study on D-glucosamine Promoted Regioselective Sulfenylation of Indoles Catalyzed by Copper. *New J. Chem.* **2017**, *41*, 13175−13180.

(11) (a) Savarin, C.; Srogl, J.; Liebeskind, L. S. A Mild, Nonbasic Synthesis of Thioethers. The Copper-catalyzed Coupling of Boronic Acids with *N*-Thio(alkyl, aryl, heteroaryl)imides. *Org. Lett.* **2002**, *4*, 4309−4312. (b) Yoshida, S.; Sugimura, Y.; Hazama, Y.; Nishiyama, Y.; Yano, T.; Shimizu, S.; Hosoya, T. A Mild and Facile Synthesis of Aryl and Alkenyl Sulfides via Copper-catalyzed Deborylthiolation of Organoborons with Thiosulfonates. *Chem. Commun.* **2015**, *51*, 16613−16616. (c) Grassl, S.; Hamze, C.; Koller, T. J.; Knochel, P. Copper-Catalyzed Electrophilic Thiolation of Organozinc Halides by Using *N*-Thiophthalimides Leading to Polyfunctional Thioethers. *Chem-Eur. J.* **2019**, *25*, 3752−3755. (d) Kang, J. C.; Li, Z. H.; Chen, C.; Dong, L. K.; Zhang, S. Y. Paired Electrolysis Enabled Ni-Catalyzed Unconventional Cascade Reductive Thiolation Using Sulfinates. *J. Org. Chem.* **2021**, *86*, 15326−15334. (e) Wang, Y.; Zhang, F.; Wang, Y.; Pan, Y. Electrochemistry Enabled Nickel-Catalyzed Selective C−S Bond Coupling Reaction. *Eur. J. Org. Chem.* **2022**, e202101462 .

(12) Lovering, F.; Bikker, J.; Humblet, C. *J. Med. Chem.* **2009**, *52*, 6752−6756.

(13) (a) Fang, Y.; Rogge, T.; Ackermann, L.; Wang, S. Y.; Ji, S. J. Nickel-Catalyzed Reductive Thiolation and Selenylation of Unactivated Alkyl Bromides. *Nat. Commun.* **2018**, *9*. (c) Li, J.; Wang, S. Y.; Ji, S. J. Nickel-Catalyzed Thiolation and Selenylation of Cycloketone Oxime Esters with Thiosulfonate or Seleniumsulfonate. *J. Org. Chem.* **2019**, *84*, 16147−16156.

(14) For reviews on nickel-catalyzed 1,2-dicarbofunctionalization of unactivated alkenes: (a) Derosa, J.;

https://doi.org/10.26434/chemrxiv-2023-ft0bn **ORCID:** https://orcid.org/0000-0003-2767-6556 Content not peer-reviewed by ChemRxiv. **License:** CC BY-NC-ND 4.0

Apolinar, O.; Kang, T.; Tran, V. T.; Engle, K. M. Recent Developments in Nickel-Catalyzed Intermolecular Dicarbofunctionalization of alkenes. *Chem. Sci.* **2020**, *11*, 4287−4296; (b) Diccianni, J.; Lin, Q.; Diao, T. Mechanisms of Nickel-Catalyzed Coupling Reactions and Applications in Alkene Functionalization. *Acc. Chem. Res.* **2020**, *53*, 906−919. (c) Qi, X.; Diao, T., Nickel-Catalyzed Dicarbofunctionalization of Alkenes. *ACS Catal.* **2020,** *10*, 8542−8556. (d) Giri, R.; Kc, S., Strategies Toward Dicarbofunctionalization of Unactivated Olefins by Combined Heck Carbometalation and Cross-Coupling. *J. Org. Chem.* **2018,** *83*, 3013−3022; (e) Zhu, S.; Zhao, X.; Li, H.; Chu, L. Catalytic Three-Component Dicarbofunctionalization Reactions Involving Radical Capture by Nickel. *Chem. Soc. Rev.* **2021**, *50*, 10836−10856; (f) Wickham, L. M.; Giri, R., Transition Metal (Ni, Cu, Pd)-Catalyzed Alkene Dicarbofunctionalization Reactions. *Acc. Chem. Res.* **2021,** *54*, 3415−3437.

(15) Selected examples under Ni(0)/Ni(II) catalytic cycle: (a) Derosa, J.; Tran, V. T.; Boulous, M. N.; Chen, J. S.; Engle, K. M. Nickel-Catalyzed β,γ-Dicarbofunctionalization of Alkenyl Carbonyl Compounds via Conjunctive Cross-Coupling. *J. Am. Chem. Soc.* **2017**, *139*, 10657−10660; (b) Li, W.; Boon, J. K.; Zhao, Y. Nickel-Catalyzed Difunctionalization of Allyl Moieties Using Organoboronic Acids and Halides with Divergent Regioselectivities. *Chem. Sci.* **2018**, *9*, 600−607; (c) Derosa, J.; Kleinmans, R.; Tran, V. T.; Karunananda, M. K.; Wisniewski, S. R.; Eastgate, M. D.; Engle, K. M. Nickel-Catalyzed 1,2-Diarylation of Simple Alkenyl Amides. *J. Am. Chem. Soc.* **2018**, *140*, 17878−17883; (d) Basnet, P.; Kc, S.; Dhungana, R. K.; Shrestha, B.; Boyle, T. J.; Giri, R. Synergistic Bimetallic Ni/Ag and Ni/Cu Catalysis for Regioselective γ,δ-Diarylation of Alkenyl Ketimines: Addressing β-H Elimination by in situ Generation of Cationic Ni(II) Catalysts. *J. Am. Chem. Soc.* **2018**, *140*, 15586−15590. (e) Apolinar, O.; Kang, T.; Alturaifi, T. M.; Bedekar, P. G.; Rubel, C. Z.; Derosa, J.; Sanchez, B. B.; Wong, Q. N.; Sturgell, E. J.; Chen, J. S.; Wisniewski, S. R.; Liu, P.; Engle, K. M. Three-Component Asymmetric Ni-Catalyzed 1,2-Dicarbofunctionalization of Unactivated Alkenes via Stereoselective Migratory Insertion. *J. Am. Chem. Soc.* **2022**, *144*, 19337–19343.

(16) Selected examples under Ni(I)/Ni(III) catalytic cycle: (a) Logan, K. M.; Sardini, S. R.; White, S. D.; Brown, M. K. Nickel-Catalyzed Stereoselective Arylboration of Unactivated Alkenes. *J. Am. Chem. Soc.* **2018**, *140*, 159−162; (b) Derosa, J.; van der Puyl, V. A.; Tran, V. T.; Liu, M. Y.; Engle, K. M. Directed Nickel-Catalyzed 1,2-Dialkylation of Alkenyl Carbonyl Compounds. *Chem. Sci.* **2018**, *9*, 5278−5283; (c) van der Puyl, V. A.; Derosa, J.; Engle, K. M. Directed, Nickel-catalyzed Umpolung 1,2-Carboamination of Alkenyl Carbonyl Compounds. *ACS Catal.* **2019**, *9*, 224−229; (d) Kang, T.; Kim, N.; Cheng, P. T.; Zhang, H.; Foo, K.; Engle, K. M. Nickel-Catalyzed 1,2-Carboamination of Alkenyl Alcohols. *J. Am. Chem. Soc.* **2021**, *143*, 13962−13970; (e) Dhungana, R. K.; Aryal, V.; Niroula, D.; Sapkota, R. R.; Lakomy, M. G.; Giri, R. Nickel-Catalyzed Regioselective Alkenylarylation of γ,δ-Alkenyl Ketones via Carbonyl Coordination. *Angew. Chem. Int. Ed.* **2021**, *60*, 19092−19096. (f) Kang, T.; González, J. M.; Li, Z.-Q.; Foo, K.; Cheng, P. T. W.; Engle, K. M. Alkene Difunctionalization Directed by Free Amines: Diamine Synthesis via Nickel-Catalyzed 1,2-Carboamination. *ACS Catal.* **2022**, *12*, 3890–3896.

(17) (a) Li, Z.-Q.; Cao, Y.; Kang, T.; Engle, K. M. Electrophilic Sulfur Reagent Design Enables Directed *syn*-Carbosulfenylation of Unactivated Alkenes. *J. Am. Chem. Soc.* **2022**, *144*, 7189–7197. (b) Li, Z.-Q.; He, W.-J.; Ni, H.-Q.; Engle, K. M. Directed, Nickel-Catalyzed 1,2-Alkylsulfenylation of Alkenyl Carbonyl Compounds. *Chem. Sci.* **2022**, *13*, 6567–6572.

(18) For a review on the role of quinones in palladium catalysis: Vasseur, A.; Muzart, J.; Le Bras, J. Ubiquitous Benzoquinones, Multitalented Compounds for Palladium-Catalyzed Oxidative Reactions. *Eur. J. Org. Chem*. **2015**, 4053–4069.

(19) For a book chapter see: Popp, B. V.; Stahl, S. S. **2006**. Palladium-Catalyzed Oxidation Reactions: Comparison of Benzoquinone and Molecular Oxygen as Stoichiometric Oxidants. In: Meyer, F., Limberg, C. (eds) Organometallic Oxidation Catalysis. Topics in Organometallic Chemistry, vol 22. Springer, Berlin, Heidelberg. https://doi.org/10.1007/3418_039. For selected examples on alkene functionalization: (a) Delcamp, J. H.; Brucks, A. P.; White, M. C. A General and Highly Selective Chelate-Controlled Intermolecular Oxidative Heck Reaction *J. Am. Chem. Soc*. **2008**, *130*, 11270–11271. (b) DeLuca, R. J.; Sigman, M. S. Anti-Markovnikov Hydroalkylation of Allylic Amine Derivatives via a Palladium-Catalyzed Reductive Cross-Coupling Reaction *J. Am. Chem. Soc*. **2011**, *133*, 11454–11457. (c) Liu, Z.; Ni, H.-Q.; Zeng, T.; Engle, K. M. Catalytic Carbo- and Aminoboration of Alkenyl Carbonyl Compounds via Five- and Six-Membered Palladacycles. *J. Am. Chem. Soc.* **2018**, *140*, 3223–3227. (d) Yang, X.; Li, X.; Chen, P.; Liu, G. Palladium(II)-Catalyzed Enantioselective Hydrooxygenation of Unactivated Terminal Alkenes. *J. Am. Chem. Soc*. **2022**, *144*, 7972–7977.

(20) (a) Grennberg, H.; Gogoll, A.; Bäckvall, J. E. Acid-induced Transformation of Palladium(0)-Benzoquinone Complexes to Palladium (II) and Hydroquinone. *Organometallics* **1993**, *12*, 1790–1793. (b) Chen, X.; Li, J.-J.; Hao, X.-S.; Goodhue, C. E.; Yu, J.-Q. Palladium-Catalyzed Alkylation of Aryl C−H Bonds with sp^3 Organotin Reagents Using Benzoquinone as a Crucial Promoter. *J. Am. Chem. Soc*. **2006**, *128,* 78–79. (c) Hull, K. L.; Sanford, M. S. Mechanism of Benzoquinone-Promoted Palladium-Catalyzed Oxidative Cross-Coupling Reactions *J. Am. Chem. Soc.* **2009**, *131*, 9651–9653. (d) Salazar, C. A.; Flesch, K. N.; Haines, B. E.; Zhou, P. S.; Musaev, D. G.; Stahl, S. S. Tailored Quinones Support High-Turnover Pd Catalysts for Oxidative C–H Arylation with O_2. *Science* **2020**, *370*, 1454–1460. (e) Bruns, D. L.; Musaev, D. G.; Stahl, S. S. Can Donor Ligands Make $Pd(OAc)_2$ a Stronger Oxidant? Access to Elusive Palladium(II) Reduction Potentials and Effects of Ancillary Ligands via Palladium(II)/Hydroquinone Redox Equilibria. *J. Am. Chem. Soc.* **2020**, *142*, 19678–19688.

(21) (a) Tran, V. T.; Li, Z.-Q.; Apolinar, O.; Derosa, J.; Wisniewski, S. R.; Joannou, M. V.; Eastgate, M. D.; Engle, K. M. Ni(COD)(DQ): An Air-Stable 18-Electron Nickel(0)–Olefin Precatalyst. *Angew. Chem. Int. Ed*. **2020**, *59*, 7409–7413. (b) Tran, V. T.; Kim, N.; Rubel, C. Z.; Wu, X.; Kang, T.; Jankins, T. C.; Li, Z.-Q.; Joannou, M. V.; Ayers, S.; Gembicky, M.; Bailey, J.; Sturgell, E. J.; Sanchez, B. B.; Chen, J. S.; Lin, S.; Eastgate, M. D.; Wisniewski, S. R.; Engle, K. M. Structurally Diverse Bench-Stable Nickel(0) Pre-Catalysts: A Practical Toolkit for In Situ Ligation Protocols. *Angew. Chem. Int. Ed.* **2023**, *62*, e202211794.

(22) a) Jang, Y.; Lindsay, V. N. G. Synthesis of Cyclopentenones with Reverse Pauson–Khand Regiocontrol via Ni-Catalyzed C–C Activation of Cyclopropanone. *Org. Lett.* **2020**, *22*, 8872−8876. (b) Reilly, S. W.; Lam, Y.; Ren, S.; Strotman, N. A. Late-Stage Carbon Isotope Exchange of Aryl Nitriles through Ni-Catalyzed C–CN Bond Activation. *J. Am. Chem. Soc.* **2021**, *143*, 4817−4823. (c) Cho, I. Y.; Kim, W. G.; Jeon, J. H.; Lee, J. W.; Seo, J. K.; Seo, J.; Hong, S. Y. Nickelocene as an Air- and Moisture-Tolerant Precatalyst in the Regioselective Synthesis of Multisubstituted Pyridines. *J. Org. Chem*. **2021**, *86*, 9328−9343. (d) Li, Y.; Shao, Q.; He, H.; Zhu, C.; Xue, X.-S.; Xie, J. Highly Selective Synthesis of All-Carbon Tetrasubstituted Alkenes by Deoxygenative Alkenylation of Carboxylic Acids. *Nat. Commun.* **2022**, *13*, 10. (e) Roediger, S.; Leutenegger, S. U.; Morandi, B. Nickel-Catalysed Diversification of Phosphine Ligands by Formal Substitution at Phosphorus. *Chem. Sci*. **2022**, *13*, 7914−7919. (f) You, T.; Li, J. Ni(cod)(duroquinone)-Catalyzed C–N Cross-Coupling for the Synthesis of N,N-Diarylsulfonamides. *Org. Lett*. **2022**, *24*, 6642−6646. (g) Orchanian, N. M.; Guizzo, S.; Steigerwald, M. L.;

https://doi.org/10.26434/chemrxiv-2023-ft0bn **ORCID:** https://orcid.org/0000-0003-2767-6556 Content not peer-reviewed by ChemRxiv. **License:** CC BY-NC-ND 4.0

Nuckolls, C.; Venkataraman, L. Electric-Field-Induced Coupling of Aryl Iodides with a Nickel(0) Complex. *Chem. Commun*. **2022**, *58*, 12556−12559. (h) Tao, S.-C.; Meng, F.-C.; Wang, T.; Zheng, Y.-L. Ni-Catalyzed Arylation of Alkynes with Organoboronic Acids and Aldehydes to Access Stereodefined Allylic Alcohols. *Chem. Sci.* **2023**, *14*, 2040−2045.
(23) (a) Jain, R.; Kabir, K.; Gilroy, J. B.; Mitchell, K. A.; Wong, K. C.; Hicks, R. G. High-Temperature Metal-Organic Magnets. *Nature* **2007**, *445*, 291−294. (b) Huynh, M. T.; Anson, C. W.; Cavell, A. C.; Stahl, S. S.; Hammes-Schiffer, S. Quinone 1 e^- and 2 e^-/2 H^+ Reduction Potentials: Identification and Analysis of Deviations from Systematic Scaling Relationships. *J. Am. Chem. Soc.* **2016**, *138*, 15903−15910.
(24) (a) Blacquiere, J. M. Structurally-Responsive Ligands for High-Performance Catalysts. *ACS Catal.* **2021**, *11*, 5416–5437. (b) Orsino, A. F.; Moret, M.-E. Nickel-Catalyzed Alkyne Cyclotrimerization Assisted by a Hemilabile Acceptor Ligand: A Computational Study. *Organometallics* **2020**, *39*, 1998–2010. (c) Shao, H.; Chakrabarty, S.; Qi, X.; Takacs, J. M.; Liu, P. Ligand Conformational Flexibility Enables Enantioselective Tertiary C–B Bond Formation in the Phosphonate-Directed Catalytic Asymmetric Alkene Hydroboration. *J. Am. Chem. Soc.* **2021**, *143*, 4801–4808. (d) Font, P.; Valdés, H.; Guisado-Barrios, G.; Ribas, X. Hemilabile MIC^N Ligands Allow Oxidant-Free Au(I)/Au(III) Arylation-Lactonization of γ-Alkenoic Acids. *Chem. Sci.* **2022**, *13*, 9351−9360. (e) Wang, P.-F.; Yu, J.; Guo, K.-X.; Jiang, S.-P.; Chen, J.-J.; Gu, Q.-S.; Liu, J.-R.; Hong, X.; Li, Z.-L.; Liu, X.-Y. Design of Hemilabile N,N,N-Ligands in Copper-Catalyzed Enantioconvergent Radical Cross-Coupling of Benzyl/Propargyl Halides with Alkenylboronate Esters. *J. Am. Chem. Soc.* **2022**, *144*, 6442–6452.
(25) Conformational search was performed using CREST and GFN2-xTB. All low-energy conformers were then fully optimized by DFT at the (U)ωB97X-D/6-311+G(d,p)–SDD(Ni)/SMD(THF)//(U)B3LYP-D3(BJ)/6-31G(d)–SDD(Ni) level of theory. See SI for computational details.
(26) (a) Foster, a. J.; Weinhold, F. Natural Hybrid Orbitals. *J. Am. Chem. Soc.* **1980**, *102*, 7211–7218. (b) Carpenter, J.; Weinhold, F. Analysis of the Geometry of the Hydroxymethyl Radical by the "Different Hybrids for Different Spins" Natural Bond Orbital Procedure. *J. Mol. Struct: Theochem.* **1988**, *169*, 41−62.
(27) Chakarawet, K.; Harris, T. D.; Long, J. R. Semiquinone Radical-Bridged M_2 (M= Fe, Co, Ni) Complexes with Strong Magnetic Exchange Giving Rise to Slow Magnetic Relaxation. *Chem. Sci.* **2020**, *11*, 8196–8203.
(28) Tendera, L.; Schaub, T.; Krahfuss, M. J.; Kuntze-Fechner, M. W.; Radius, U. Large vs. Small NHC Ligands in Nickel(0) Complexes: The Coordination of Olefins, Ketones and Aldehydes at [Ni(NHC)$_2$]. *Eur. J. Inorg. Chem.* **2020**, *33*, 3194–3207.
(29) CCDC 2304663 and 2304664 contain the supplementary crystallographic data for this paper. These data can be obtained free of charge from the Cambridge Crystallographic Data Centre via www.ccdc.cam.ac.uk/data_request/cif. CCDC:,

https://doi.org/10.26434/chemrxiv-2023-ft0bn **ORCID:** https://orcid.org/0000-0003-2767-6556 Content not peer-reviewed by ChemRxiv. **License:** CC BY-NC-ND 4.0

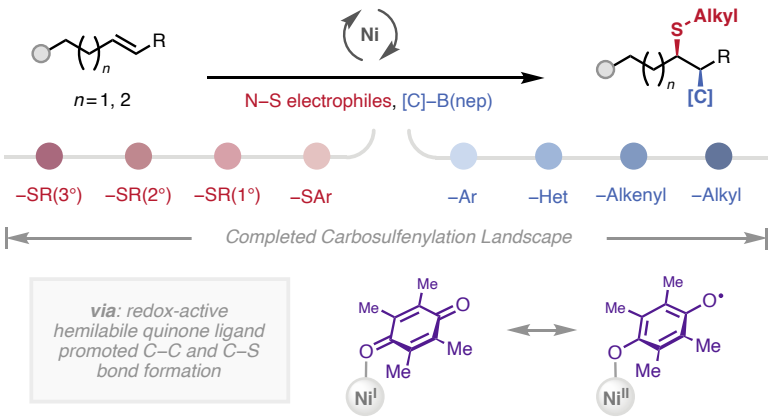

https://doi.org/10.26434/chemrxiv-2023-ft0bn **ORCID:** https://orcid.org/0000-0003-2767-6556 Content not peer-reviewed by ChemRxiv. **License:** CC BY-NC-ND 4.0